

## 2D and 3D Resistivity Imaging for Soil Site Investigation

**Dr. Hussein H. Karim**

Building and Construction Engineering Department, University of Technology/Baghdad

Email: [husn\\_irq@yahoo.com](mailto:husn_irq@yahoo.com)

**Dr. Dr. Mahmoud R. AL- Qaissy**

Building and Construction Engineering Department, University of Technology/ Baghdad

**Nadia A. Aziz**

Received on: 27/1/2013

&

Accepted on: 3/10/2013

### ABSTRACT

Electrical Resistivity Imaging (ERI) method is one of the most promising techniques which is well suited to applications in the fields of geohydrology, environmental science and engineering. The present work is aimed to show the efficiency of 2D Electrical Resistivity Imaging (ERI) and Induced Polarization (IP) in probing the subsurface soil for site investigation and differentiating the clayey soil layers as it is a common practice to measure the IP sounding along with resistivity for correct interpretation of field data. The study has demonstrated the practical application of 2D ERI and IP tomography along 7 lines using Wenner- Schlumberger array. The data analysis comprises of 2D inversions using the RES2DINV software, thus 2D electrical resistivity and IP imaging sections have been obtained. The depth of investigation was 4 m, and resistivity values range from <1 to 292 ohm.m. Two electrical layers were recognized: the upper layer with high resistivity (7-71 ohm.m) represents the loamy soil extends to a depth around 1.3 m; and the second layer with low resistivity (<1-9 ohm.m) represents the clayey layer. Some anomalous low and high electric zones are appeared reflecting the inhomogeneity in deposits. The IP values are ranging from -2 to 15 mV/V showing good confirmation with resistivity data, where high chargeability are associated with low resistivity. The study reveals that combining IP with resistivity surveys is recommended since IP is, sometimes, very effective in relieving ambiguity in interpretation.

**Keywords:** 2D Electrical resistivity imaging (2D-ERI); IP Imaging; Chargeability; Clayey Soil; Site Investigation

### المقاومة النوعية التصويرية ثنائية وثلاثية الأبعاد للتحري الموقعي للتربة

#### الخلاصة

تم تطبيق طريقة المقاومة النوعية الكهربائية التصويرية (ERI) لإنتاج معلومات مستمرة من تحت سطح الأرض ولجس أمتار عدة لما تحت السطح لتعطي قاعدة بيانات ثلاثية الأبعاد (3D). لقد تم مسح 14 خطاً متوازيًا و 3 خطوط متعامدة عن طريق تطبيق المسح ثنائي الأبعاد (2D) والتي يتم جمعها لخلق مجموعة بيانات ثلاثية

الأبعاد باستخدام ترتيب فنر - شلمبرجير. كما استخدمت قياسات جس الأستقطاب المستحث (IP) جنباً إلى جنب مع المقاومة النوعية على طول بعض الخطوط باستخدام نفس الترتيب من أجل تكامل البيانات الحقلية. في كل من المقاومة النوعية والأستقطاب المستحث، بلغ عمق التحري ما بين (4-8 m). تتراوح قيم المقاومة النوعية ما بين ( $126 \text{ ohm.m}$  to  $<1$ ). تم التعرف على طبقتين كهربائيتين: العليا ذات مقاومة نوعية عالية ( $126 \text{ ohm.m}$  to  $9$ ) تمثل طبقة الطين الرطبة الطموية إلى عمق حوالي (1 m); والثانية ذات مقاومة نوعية واطئة ( $9 \text{ ohm.m}$  to  $1$ ) تمثل طبقة الطين الرطب- الجاف. تتراوح قيم IP ما بين ( $17 \text{ mV/V}$  to  $-2$ ) مع شاحنية عالية (مقاومة نوعية واطئة) للطين اللين. بينما الشاحنية الواطئة تطابق المقاومة النوعية العالية في مقاطع المقاومة النوعية لنفس الموقع. تظهر أنطقة الطين اللين قابلية شحنية (chargeability) عالية (بحدود  $4.3 \text{ mV/V}$  to  $2.5$ ) في الأعماق القريبة من السطح إلى عمق حوالي (2.5 m). تظهر بعض النشرات قابلية شحنية واطئة جدا ( $0.04 \text{ mV/V}$ ) والتي تشير إلى المحتوى المائي العالي بسبب عملية الري. تعتبر قياسات IP مكمل جيد لحل الغموض في التفسير طالما يعد مؤشر على المحتوى الطيني. تعكس صور المقاومة النوعية ثلاثية الأبعاد (3D) وضوحاً أكثر لتوزيع المقاومة النوعية التي تعطي 14 شريحة عمق مختلفة للنموذج المقدر مع فاصل عمق حوالي (0.75 m). وأظهرت المقاطع التصويرية ثلاثية الأبعاد اتفاق جيد مع البيانات التي تم الحصول عليها من حفر الآبار المتوفرة في المنطقة. أوصت هذه الدراسة إلى تنفيذ قياسات المقاومة الكهربائية 2D و 3D جنباً إلى جنب مع اختبارات التربة الهندسية للحصول على أفضل توصيف للتربة تحت السطحية قبل الشروع في أي نوع من أنواع العمل الإنشائي.

## INTRODUCTION

Electrical resistivity techniques have been used in many geological formations for characterizing the subsurface for many years. In the earlier applications, the technique was considered to be very labour intensive. The development of the 2-D multi-electrode surveys has been able to reduce this aspect of the survey [1]. Electrical resistivity imaging (ERI) is considered to be the most applicable technique that has been used for many decades in geological, geotechnical, hydrogeological, environmental and archeological investigations. Many works have been done to establish a relationship between soil engineering test and ERI data [2, 3, and 4]. Another important advantage of ERI is that it produces continuous information of the subsurface and probes into several meters below the surface. Survey design and layout strategies that produce optimum information using different Electrical Resistivity Imaging (ERI) configurations and set up in different geological settings have been the topic of several studies (e.g., Alumbaugh and Newman, 1999 [5]; Stummer et al., 2004 [6]; Ayolabi et al., 2009) [7].

The use of 2D and 3D resistivity surveys has enabled us to map complex geological structures that were not previously possible with conventional 1D resistivity surveys Figure (1). With the newly introduced technical developments, equipment, automatic inversion techniques and computer hardware such surveys can now be routinely carried out by small firms. Most geological structures are three dimensional (3D) in nature. A 3D interpretation resistivity model Figure (1c) is an active area of investigation at the present time.

It has been stated that 2D ERI method is cost effective, efficient and less time consuming in geotechnical investigation than most geotechnical tests [8]. Because of simplicity in field implementation, 2D resistivity surveys are still used in most investigations; however, they can lead to distorted and misleading results in heterogeneous areas. Recently, Bentley and Gharibi (2004) [9] demonstrated distortions in 2D images and described a 3D ERI survey design in which orthogonal

sets of 2D resistivity survey lines are combined to create a 3D dataset. The 2D lines are jointly inverted to produce a 3D image. The study concluded that appropriately designed 3D arrays can be used efficiently for site characterization.

The most commonly used arrays in the 2D electrical imaging surveys are conventional arrays such as the Wenner, Schlumberger or dipole-dipole arrays. These arrays are often well understood in terms of their depths of investigations, lateral and vertical resolution and signal- to- noise ratios [10].

The present work is aimed at showing the efficiency of 2D and 3D Electrical Resistivity Imaging (ERI) in probing the subsurface soil for site investigation.

### ELECTRICAL RESISTIVITY– BASIC THEORY

The theory of electrical resistivity suggests that electric current flows in the subsurface soil by electrolytic rather than electronic processes [11]. The resistivity measurements are normally made by injecting current into the ground through two current electrodes (C1 and C2), and measuring the resulting voltage difference at two potential electrodes (P1 and P2) over a distance. The current and potential electrodes are generally arranged in a linear pattern.

The Electrical Resistivity Imaging concept is based on the relation that normally gives a resistance value

$$V = R \times I \quad \dots (1)$$

in which the current passing through the ground (I), and the corresponding change in potential ( $\Delta V$ ). There is another relationship that defines the resistance (R) as a function of geometry of a resistor and the resistivity of the cylindrical-shaped body:

$$R = \frac{\rho \times L}{A} \quad \dots (2)$$

By rearranging Equation (2), the resistivity can be expressed as:

$$\rho = \frac{R \times A}{L} \quad \dots (3)$$

So in practice the apparent resistivity value is calculated by

$$\rho_a = kR \quad \dots (4)$$

The apparent resistivity  $\rho_a$  is the bulk average resistivity of all soils and rocks influencing the flow of current [12, 13].

From the current (I) and voltage (V) values, an apparent resistivity ( $\rho_a$ ) value is calculated from dividing the measured potential difference by the applied current times the geometric factor ( $k$ ),

$$\rho_a = k \left( \frac{V}{I} \right) \quad \dots (5)$$

Where  $k$  is the geometric factor which depends on the arrangement of the four electrodes. Thus, a factor that defines the ease for electrical current to flow through the media is known as resistivity ( $\rho$ ). Resistivity is an internal parameter of the material through which current is compelled to flow and describes how easily this material can transmit an electrical current. High values of resistivity imply that the material making up the medium is very resistant to the flow of electricity. Low values of resistivity show that the material making up the medium transmits electrical current very easily.

Hence, porosity is the major control of resistivity of rocks, and that resistivity generally increases as porosity decreases. Porosity and cementation, on the other hand, are related. It then means that electrical resistivity could be used to determine the degree of cementation to better characterize the subsurface soil for engineering structures [7].

## **METHODOLOGY**

### **2D and 3D Resistivity Surveys**

Most geological structures are three dimensional (3D) in nature. A 3D interpretation resistivity model as shown in Figure 1c is an active area of investigation at the present time. The 3D resistivity imaging method is probably the best method to map 3D structures. But its usage is not as routinely as the 2D survey. This is because of the higher cost of a 3D survey for covering a large survey area. However, there are two recent developments that probably make 3D survey more cost-effective choice in the near future. Firstly, a multi-channel resistivity-meter which makes more than one reading at the same time can significantly reduce the survey time. The multi-electrode or multi-channel resistivity imaging systems are now readily available and so many researchers are carrying out 3D resistivity surveys. Moreover, new faster microcomputers can enhance the inversion of huge data sets [14].

The most common way to build a 3D data set is by applying a number of 2D survey lines and then combines them into 3D data set. These lines have to be parallel to each other with constant line spacing. In the field, there have to be a set of survey lines with dimensions both in the  $x$  and  $y$  directions. Yang and Lagmanson (2006) [15] found that to get the best 3D resistivity survey it has to use a large number of cross-line measurements with the true 3D survey because it offers a better subsurface resolution compared to the pseudo 3D survey. But even if the pseudo 3D survey run out without any cross-line measurements, it is still an acceptable choice to a true 3D survey as far as the line spacing is equal to or less than twice the electrode spacing. Therefore, in term of any project that has limited number of electrodes it is possible now to obtain a high resolution result from the 3D survey [10].

To be correctly interpreted, the measured integrated values must be converted so they can then be correlated to the resistivity parameter and to other soil characteristics. This conversion can be made by inversion software and the results are then called "inverted resistivities". The RES2DINV software was used in this case to calculate a distribution map of inverted resistivity. At each point of the map, the inverted resistivity value corresponds to the value of resistivity at that location, without any integration. Final 2-D and 3-D plots were obtained after linear interpolation.

## SURVEY DESIGN AND DATA ACQUISITION

### Field work, Equipment of Multi-Electrode Survey

The ABEM Terrameter SAS 4000 (Signal Averaging System 4000) was the equipment used for all the data collection for this research work, consecutive readings were taken automatically, and the results were averaged continuously Figure (2). The main features include a 64 electrode unrestricted switching in a compact, battery operated unit with a robust waterproof design for reliable operation in harsh environment. The ABEM was very effective in the area and generally did not encounter a lot of problems during the field data collection. There were particular times when the equipment was affected by the high temperature, but this was very limited.

The site of work was carried out in the football field of the University of Technology in Baghdad Figure ( 3). The resistivity imaging survey was conducted through more than 3-months between February 27, 2012 and May 3, 2012. The dimension of the site is 40 m by 20 m. The measurements were made along 14 south-north parallel lines and 3 west-east parallel lines.

The research project involved a 41 electrode SAS 4000 multi-electrode resistivity system to collect the apparent resistivity data. The 41 electrodes are on two interconnect electrode cables with 20 electrodes each.

The resistivity imaging for vertical sections (Lines A to N), trending from south to north, was conducted with 1m electrode spacing using the Wenner-Schlumberger array. The total length of the survey line was 40 m. The line spacing was 1.5 m for all lines, except for the last space (M-N) where it was 2 m. While the horizontal sections (Lines 1, 3 and 7), trending from west to east, was conducted with 0.5 m electrode spacing and total length 20 m using the same array Figure (4).

A general 2D profile acquisition of the resistivity data is fairly straightforward. The data was processed and inverted using RES2DINV software. The program generates the inverted resistivity-depth image for each profile line. The soil type has been identified according to typical ranges of electrical resistivity for soils (e.g. Loke, 2012 [14]) in addition to the use of IP values and the information available from boreholes in the study area.

## 2D ELECTRICAL RESISTIVITY IMAGING SURVEY

### S-N Resistivity Sections

For 2D, the survey is conducted along 14 parallel inversion resistivity sections trending from S to N direction with total length of 40 m. The depth of the investigation ranges between 7.58 m (for lines A to H) to 8.6 m (for lines I to N). The resistivity values vary between  $<1$  to 126 ohm.m. The RMS ranges between 2.7 to 12.2% after 7-10 iterations. The main characteristics of such sections are described as follows:

#### LINE A

The inversion resistivity section of LINE A with borehole lithology (drilled at Engineering Computer and Information Technology Department site) is shown in Figure 5. The soil profile shows top layer from the soil surface to a depth of about 1-1.5 m. This layer consists of fill material of brown sandy clayey silt with fragments

and gravels. The second layer consists of soft to medium dark brown sandy clayey silt below the fill layer, which extends to a depth ranged from 8-9 m below natural ground level with an average thickness of 8 m. The third layer consists of medium to stiff dark brown sandy-silty clay, which extends to a depth ranged from 13-13.5 m below natural ground level with an average thickness of 4 m. The fourth layer is medium to dense fine gray, fine silty-sandy gravel, which extends to the end of boring [16].

The resistivity values of this line vary between 1.7 and 36 ohm.m. The inversion resistivity image Figure (5) shows three different layers, first layer contains loam soil showing a high resistivity that ranges from 9.6 to 36 ohm.m. The intermediate layer shows resistivity values of around 4 ohm.m which may represent a thin wet sand layer. The third layer shows a low resistivity value of 2.6 ohm.m and was interpreted as a clay layer. The profile presents mainly two distinguishable zones with a high resistivity value. The highest one occurs between -12 and -4 m in the left side of the profile, from 0.2 m down to 1 m in depth, with a maximum value around 36 ohm.m. This zone is interpreted as possibly cavity to dry sand. And the second zone occurs between 6 and 10 m along the profile, from 0.2 m down to 1 m in depth, with a maximum value 23 ohm.m. This zone may represent the presence of sand to clay with cavities (voids).

#### **LINE B**

The resistivity values of this line vary between 1 to 76 ohm.m. The inversion resistivity image Figure (6) shows two different layers. The first layer contains loam soil showing a high resistivity that ranges from 12 to 76 ohm.m. The second layer shows a low resistivity values that ranges from 1 to 3.6 ohm.m and is interpreted as a clay layer. The profile presents four distinguishable zones with a high resistivity value. The highest one occurs between -12 and -4 m in the left side of the profile, from 0.2 m down to 1 m in depth, with a maximum value around 76 ohm.m. This zone may represent the presence of clay with cavity to dry sand. The second zone occurs between -12 and -4 m along the profile, from 2.5 m down to 3.7 m in depth, with a maximum value 41 ohm.m. The third zone occurs between 4 and -4 m along the profile, from 1.3 m down to 3.7 m in depth, with a maximum value 41 ohm.m. And the last zone occurs between 8 and 14 m along the profile, from 2.5 m down to 5 m in depth, with a maximum value 12.2 ohm.m. These later two zones are interpreted as sandy clay to clay with cavities.

#### **LINE C**

The resistivity values vary between 1.8 and 49 ohm.m. From the analysis of line C Figure (7), there are two different layers, first layer contains of loam soil showing a high resistivity that ranges from 7.5 to 49 ohm.m. The second layer shows a low resistivity that ranges from 1.8 to 2.9 ohm.m and was interpreted as a clay layer. The profile presents three distinguishable zones with a high resistivity value. The highest one occurs between -12 and -4 m in the left side of the profile, from 0.2 m down to 1 m in depth, with a maximum value around 49 ohm.m. This zone is interpreted as possibly cavity to dry sand for its high resistivity value. The second zone occurs between 0 and -12 m along the profile, from 2.5 m down to 3.7 m in depth, with a maximum value 7.5 ohm.m. And the third zone occurs between 6 and -12 m along the profile, from 2.5 m down to 5 m in depth, with a maximum value 7.5 ohm.m. The latter two zones may be interpreted as sand to clay with cavities.

**LINE D**

The resistivity values vary between 1 and 67.5 ohm.m. From the analysis of line D Figure (8) there are two layers, first layer contains loam soil showing a high resistivity that ranges from 11 to 67.5 ohm.m. The second layer shows the low resistivity that ranges from 1 to 3.3 ohm.m and was interpreted as a clay layer. The profile presents four distinguishable zones with a high resistivity value. The highest one occurs between -12 and -4 m in the left side of the profile, from 0.2 m down to 1 m in depth, with a maximum value around 67.5 ohm.m. This anomaly is interpreted as possibly cavity to dry sand. The second zone occurs between -6 and -14 m along the profile, from 2.5 m down to 3.7 m in depth, with a maximum value 20.2 ohm.m. It is interpreted as a presence of sand. The third zone occurs between 6 and 12 m along the profile, from 2.5 m down to 5 m in depth, with a maximum value 11 ohm.m. The last zone occurs between 4 and -4 m along the profile, from 1.3 m down to 3.7 m in depth, with a maximum value 6 ohm.m. The latter two zones may be interpreted as sandy clay to clay with cavities.

**LINE E**

The resistivity values vary between 1.1 and 37.5 ohm.m. The subsurface resistivity image along line E Figure ( 9) appears basically identical to that of LINE D and LINE C, except for few details. The same layers and zones appeared. The zone which occurs between -4 and -16 m along the profile, from 2.5 m down to 3.7 m in depth, with a maximum value 13.5 ohm.m became bigger than the previous profile.

**LINE F**

The resistivity values vary between 0.75 and 54 ohm.m Figure (10). Findings here are similar to those of lines C, D and E.

**LINE G**

The resistivity values vary between 1.8 and 69.6 ohm.m Figure (11). Again the findings are similar to those of the previous four lines which could be due to short distance between the profiles (1.5 m).

**LINES H to L**

Similar findings are assigned for Lines H, I, J, K, and L except the resistivity range values which is between <1 to 126 ohm.m Figures (12 to 16).

**LINE M**

The resistivity values vary between 1.4 and 30 ohm.m Figure (17). From the analysis of line M there are two different layers; first layer contains loam soil showing a high resistivity that ranges from 19.2 to 30 ohm.m. The second layer shows the low resistivity that ranges from 1.4 to 8 ohm.m and was interpreted as a clay layer. The profile presents distinguishable zones with a low resistivity value occurs between -12 and 12 m in the center of the profile, from 0.6 m down to 2.6 m in depth, with a value 1.4 ohm.m, these zones are interpreted as soft clay.

**LINE N**

The resistivity values from the field survey vary between 2 and 6.8 ohm.m Figure (18). It is shown in the figure below that the superficial layer extending to a depth of 1.5 m. exhibit a low resistivity value (2.9 ohm.m), in contrast to higher values of most other profiles, this may be due to accidental irrigation in the day preceding the investigation.

### W-E Resistivity Sections

For the lines (1, 3 and 7) trending from W to E, the inversion resistivity sections are with total length of 20 m. The depth of the investigation ranges between 3.75 m (for lines 1 and 3) to about 4 m (for line 7). The resistivity values vary between 0.1 to about 90 ohm.m. The RMS ranges between 1.3 to 9.9% after 2, 3 and 7 iterations. The main characteristics of these sections are described as follows:

#### LINE1

The 2D inversion resistivity pseudosection of Line 1 Figure (19a) reflects resistivity values ranging between 0.7 and 55 ohm.m. In this profile the uppermost area showed a high resistivity value ranged from 8.5 to 55 ohm.m, especially at the right side. In the deeper layer, the resistivity value ranged from 0.7 to 2.4 ohm.m, which appeared in blue color, it was interpreted as clay. A distinguishable zone with a high resistivity value was noticed in the center of the profile, from 0.1 m down to 0.5 m in depth, with a maximum value around 55 ohm.m. This anomaly is interpreted as dry sand.

The IP values for the same profile vary between -2 to 14 mV/V Figure (19b). The IP values distribution shows a homogeneous pattern except for an area located at a depth of 1.3 m down to 2.5 m with a maximum value of around 17 mV/V with high chargeability in the IP profile (compared with low resistivity values in the resistivity profile), this area was interpreted as a soft clay.

#### LINE 3

The subsurface resistivity image along Line 3 Figure (20a) appears, appears similar to that obtained from Line 1 reflecting the same appeared layers. except few details. The inversion resistivity values vary from around 0.3 to 89.5 ohm.m. The small zones with a high resistivity value (around 89.5 ohm.m) which appeared in Line 1 are present in this profile particularly in the center of the profile. These anomalies are interpreted as dry sand.

The IP values vary between -0.7 and 2.2 mV/V as shown in Figure (20b). It is noticed in this figure that the proposed clay area appeared previously in the resistivity section in blue color Figure (20a) is also shown in the IP section in yellow color with slightly higher chargeability than its surroundings, supporting its proposition as a clay area. Besides, other two main zones (brown color) appeared in both the resistivity and IP profiles at 1.5 m in depth with minimum resistivity value (0.3 ohm.m) in contrast to its accompanied high chargeability (2.3 mV/V), are interpreted as possible soft clay.

#### LINE 7

The resistivity values vary from 1.1 to 29 ohm.m. The inversion resistivity image Figure (21a) shows two different layers, the first layer is interpreted as loam soil showing high resistivity that ranges from 13 to 29 ohm.m with higher values at both ends possibly referring to the presence of small cavities or sand. The resistivity values of the second layer range from 1 to 9 ohm.m which could represent a clayey layer. This profile presents one main distinguishable zone occurring at the left side of the profile, from about 0.7 m down to 2 m in depth, with resistivity value around 3 ohm.m. This anomaly may be interpreted as possible soft clay.

The IP values vary between -1 and 15 mV/V Figure (21b). Two distinguishable zones appeared in both the resistivity and IP profiles, both with minimum resistivity



value (1 ohm.m) in contrast to its associated high chargeability (7 mV/V) which are explained as soft clay.

### 3D RESISTIVITY IMAGING ANALYSIS AND RESULTS

2D resistivity data were collected along 14 parallel lines (A to N) using a Wenner-Schlumberger configuration. Electrode cables were oriented in the x-direction with 1m spacing. Roll-along measurements using a line spacing of 1.5 m were carried out, and for extra resolution 3 tie lines (1, 3 and 7) were added using the same configuration Figure ( 4). Electrode cables were oriented in the perpendicular direction (Y-direction) with 0.5 m spacing. All data sets were merged into a single data file in order to perform a 3D inversion.

To construct a 3D resistivity data set from 2D data set, all the 2D data files were obtained and written as (TXT file) that involved 2D profile files number, names, direction and first point location. These files were converted into unified resistivity net format (filename.dat) by using RES2DINV (the option "collate data into RES3DINV format" from the "file" submenu), the program resulted in 3D data file that were opened using RES3DINV to get a 3D data file for each survey area.

Commercial inversion software packages RES3DINV was implemented for results display and analysis. This program which typically uses a smoothness-constrained least squares method is used to invert the data in terms of 3D resistivity model. In some cases, a 3D data set can be built up from a number of parallel 2D lines. The data from each 2D survey line is initially inverted independently to give 2D resistivity inversion profile.

As mentioned above, the dimension of the site is 40 m by 20 m. The measurements were made over 17 parallel lines. A total of 5077 data points for 3D image were measured. The results of the combination of 3D inversion of the data set from both directions are shown in Figure (22). The total combined 2D profiles number was 17 in both directions.

The resistivity values for this image are ranged between 1.7 and 252 ohm.m. The depth of penetration is 10 m. The total RMS after 4 iterations is 20 %. The estimated model is represented as 14 different depth slices. Their depths are 0.0-0.25 m, 0.25-0.54 m, 0.54-0.87 m, 0.87-1.25 m, 1.25-1.69 m, 1.69-2.19 m, 2.19-2.77 m, 2.77-3.43 m, 3.43-4.20 m, 4.20- 5.08 m, 5.08-6.09 m, 6.09-7.25 m, 7.25-8.59 m and 8.59-10.1 m, respectively.

The three upper (shallow) slices indicate strong variations in resistivity values (14.3 to 252 ohm.m), and these variations are attributed to heterogeneities of the soil constituents besides the variation in water content. The remaining deeper slices reveal low resistivity values varying from 1.7 to 6.9 ohm.m. Resistivity was noticed to have lower values in the fourth slice with a depth between 0.87-1.25 m. This may be due to the presence of the water table level in this depth, which is an assumption that agrees with the borehole logs results (1.2-1.3 m below the natural ground level).

## CONCLUSIONS

1. Electrical resistivity is non-destructive and can provide continuous measurements over a large range of scales. Besides, it is an attractive method for soil characterization in the contrary to regular drilling which perturbs the soil.
2. For 2D survey:
  - a. For both resistivity and IP, the depth of investigation ranges between 4 to 8 m and
  - b. Resistivity values range from  $<1$  to 126 ohm.m. Two electrical layers were recognized: the upper with high resistivity (9-126 ohm.m) represents the loamy soil to depth around 1 m; and the lower low resistivity ( $<1$ - 9 ohm.m) represents the wet to dry clayey layer.
  - c. Some distinguishable low and high electric zones are appeared reflecting the inhomogeneity in deposits. Of these, high resistivity zone (23-126 ohm.m) which possibly represent a pocket of dry sand and cavities. The other are with low resistivity ( $<1$ -11 ohm.m) represent the clayey layer.
  - d. IP measurements which be acquired simultaneously are a good complement to resolve ambiguities in the interpretation, as it is an indicator of clay content. The IP values are ranging from -2 to 17 mV/V with high chargeability (low resistivity) for soft clay. While low chargeability corresponds to high resistivity in the resistivity sections for the same site. The soft clay zones appeared with relatively high chargeability (around 2.5-4.3 mV/V) at depths from the near surface to about 2.5 m in depth. Some spreads appeared with very low chargeability (-0.04 mV/V) referring to high water content due to irrigation.
3. For 3D survey:
  - a. The depth of penetration is 10.1 m. Resistivity values varied from 1.7 to 252 ohm.m.
  - b. Fourteen different depth slices were obtained for the estimated model. Their depths are from 0.0-0.25 m to 8.59- 10.1 with average depth interval around 0.7.
  - c. The two upper (shallow) slices indicated the strong variations in resistivity values (14.3 to 252 ohm.m), which may be due to heterogeneity in the top soil constituents and water content. The remaining deeper slices revealed low resistivity values that vary between 1.7 to 6.9 ohm.m.
4. Engineering soil tests must be carried along with 2-D and 3-D electrical resistivity measurements for better characterization of the subsurface soil prior to any kinds of construction work.

## REFERENCES

- [1]. Heather, L., Stahl, A., Leberfinger, L. and Warren, J., "Electrical Imaging: A method for identifying potential collapse and other karst features near roadways", Science Applications international corporation, Middletown Pennsylvania, 1999.
- [2]. Israil, M., Pachauri, A.K., "Geophysical characterization of a land slide site in the Himalayan foothill region", Journal of Asian Earth Sciences, V. 22, pp.253-263, 2003.

- [3]. Cosenza, P., Marmet, E., Rejiba, Cui, Y.J., Tabbagh, A., Charlery, Y., "Correlations between geotechnical and electrical data: A Case Study of Garchy in France", *Journal of Applied Geophysics*, V. 60, pp.165-178, 2006.
- [4]. Gay, D. A., Morgan, F. D., Vichabian Y., Sogade, J. A., Reppert, P. and Wharton, A. E., "Investigations of andesitic volcanic debris terrains: Part 2 – Geotechnical", *Geophysics*, V. 71, B9–B15, 2006.
- [5]. Alumbaugh, D.L. and Newman, G.A., "Image appraisal for 2-D and 3-D electromagnetic inversion", In: *Proceedings of the Society of Exploration Geophysicists Annual Meeting*, New Orleans, 1998. New Orleans, Louisiana, The Society of Exploration Geophysicists, pp. 2–10, 1999.
- [6]. Stummer, P., Maurer, H. and Green, A.G., "Experimental design: Electrical resistivity data sets that provide optimum subsurface information", *Geophysics*, V. 69, No. 1, pp.120–139, 2004.
- [7]. Ayolabi, E.A., Folorunso, A. F., Adeoti, L., Matthew, S. and Atakpo, E., "2-D and 3-D Electrical Resistivity Tomography and Its Implications", A paper presented at the 4<sup>th</sup> Annual Research Conference and Fair held @ the University of Lagos, Akoka, 8<sup>th</sup> Jan, 2009, p.189, 2009. [www.ivsl.org](http://www.ivsl.org).
- [8]. Sudha, K., Israil, M., Mittal, S. and Rai, J., "Soil characterization using electrical resistivity tomography and geotechnical investigations", *Journal of Applied Geophysics*, V. 67, pp.74-79, 2009.
- [9]. Bentley, L.R. and Gharibi, M., "Two- and three-dimensional electrical resistivity imaging at a heterogeneous remediation site", *Geophysics*, V. 69, No. 3, pp. 674–680, 2004.
- [10]. Al fouzan, F.A., "Optimization strategies of electrode arrays used in numerical and field 2D resistivity imaging surveys", PhD. thesis, Universiti Sains Malaysia, pp. 25-48, 2008.
- [11]. Kearey, P., Brooks, M. and Hill I., "An introduction to geophysical exploration", Blackwell Science, Oxford, 2002.
- [12]. U.S. Army Corps of Engineers, "Engineer Manual 1110-1-1802", CECW-EG, Department of the Army, Washington, DC 20314-1000, 1995.
- [13]. Milsom, J., "Field geophysics", 3rd edition, John Wiley & Sons Ltd, 232 P., 2003.
- [14]. Loke, M.H., "Tutorial 2-D and 3-D electrical imaging, 2012. <http://www.georentals.co.uk/Lokenote.pdf>.
- [15]. Yang, X. and Lagmanson, M., "Comparison of 2D and 3D electrical resistivity imaging methods", In: *proceedings of the symposium for the application of geophysics to environmental and engineering problems (SAGEEP, 2006)*, pp. 585–590, 2006.
- [16]. Scientific and Engineering Bureau, University of Technology. "Site exploration report for the new location of Engineering Computer and Information Technology at the University of Technology", Report no. (81), 2007.

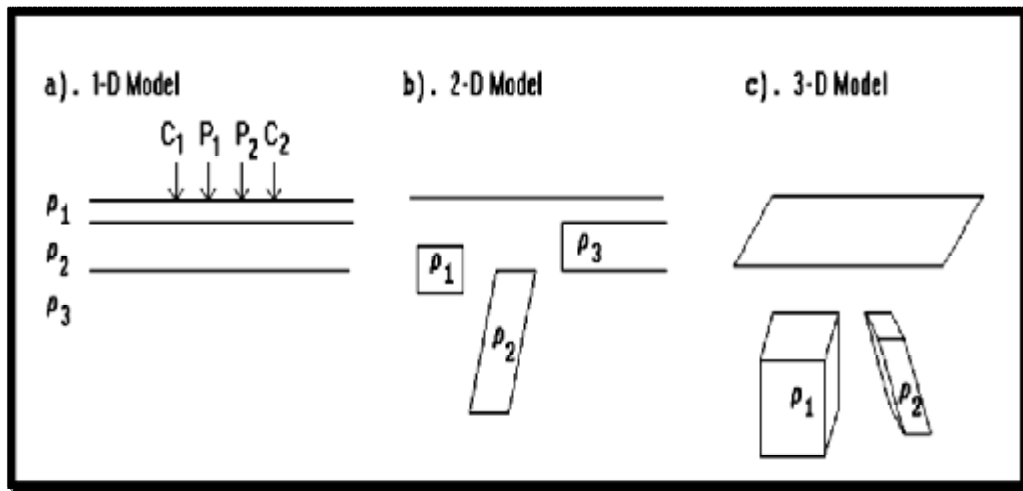


Figure (1) The three different models used in the interpretation of resistivity measurements: 1D Model, (b) 2D Model and (c) 3D Model [14].



Figure (2) ABEM Terrameter SAS 4000.



Figure (3) the surveyed site of study.



Figure (4) Geometry for 3D imaging survey.

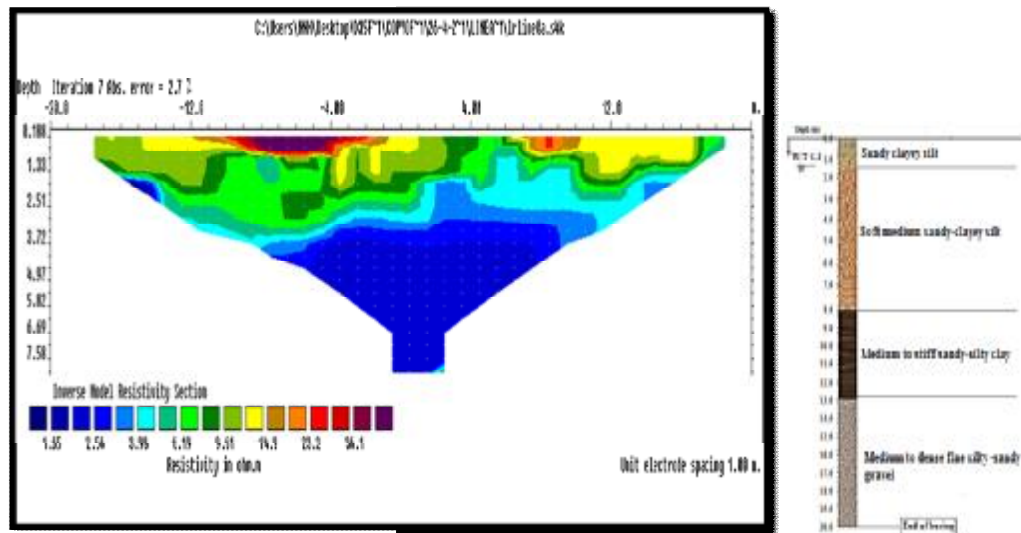


Figure (5) Inverted resistivity section for LINE A.

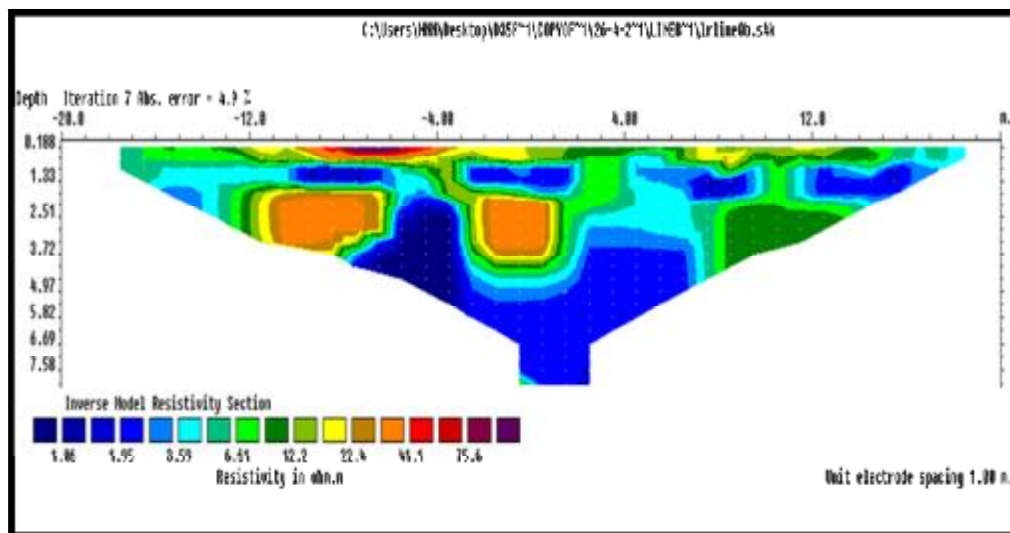


Figure (6) Inverted resistivity section for LINE B.



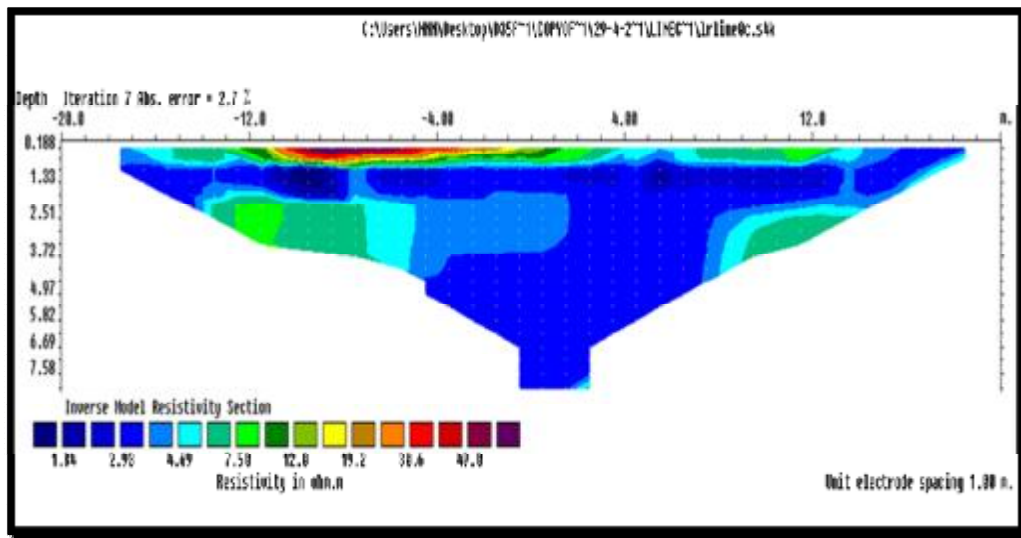


Figure (7) Inverted resistivity section for LINE C.

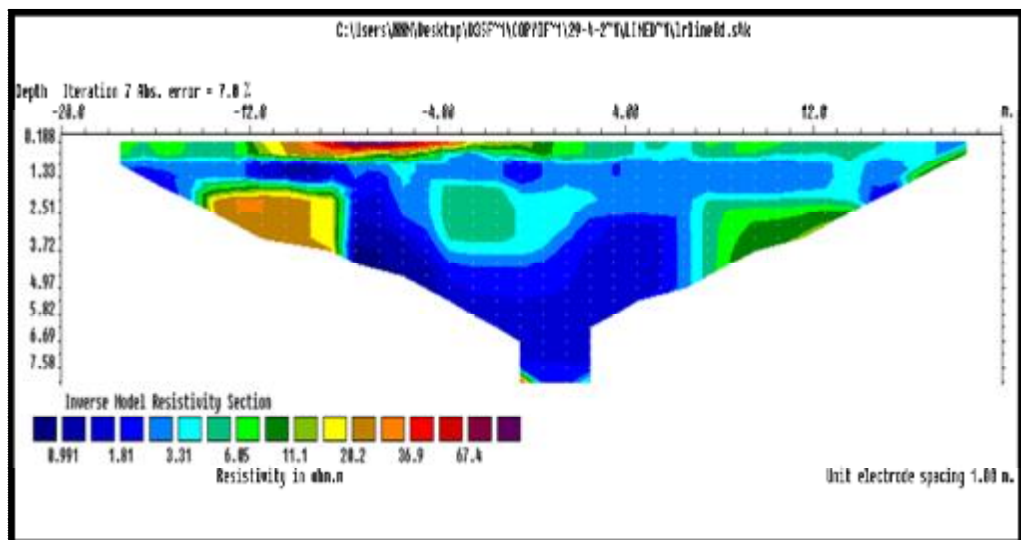


Figure (8) Inverted resistivity section for LINE D.

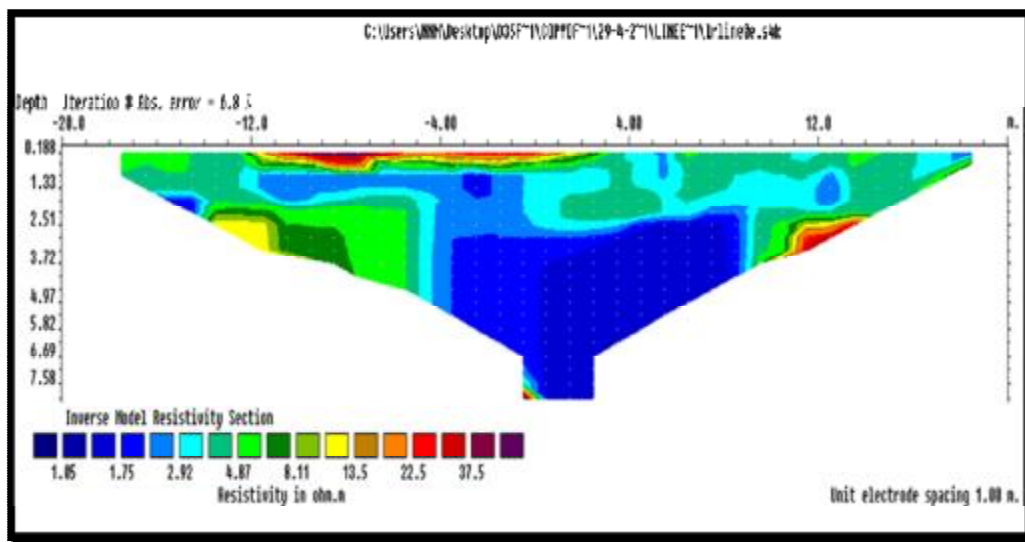


Figure (9) Inverted resistivity section for LINE E.

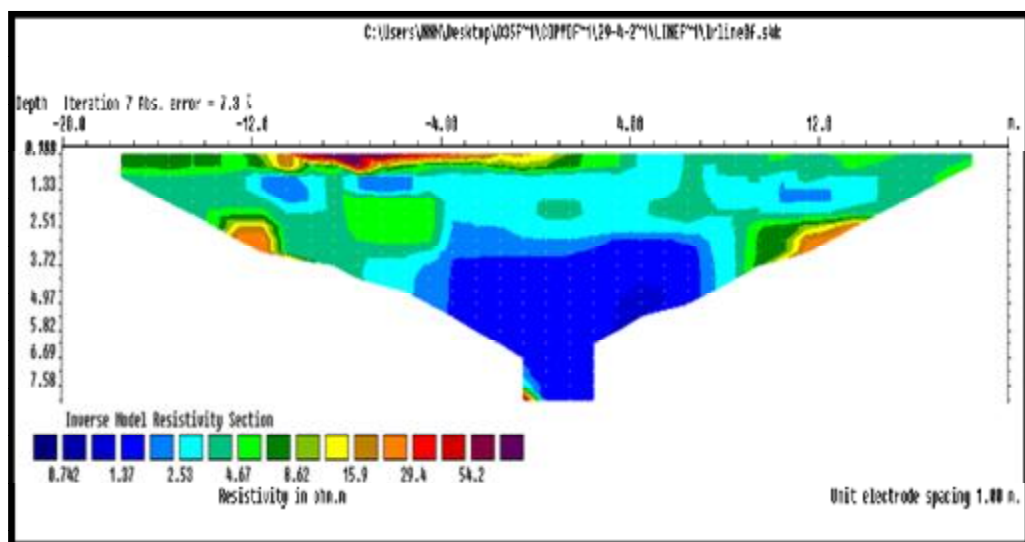
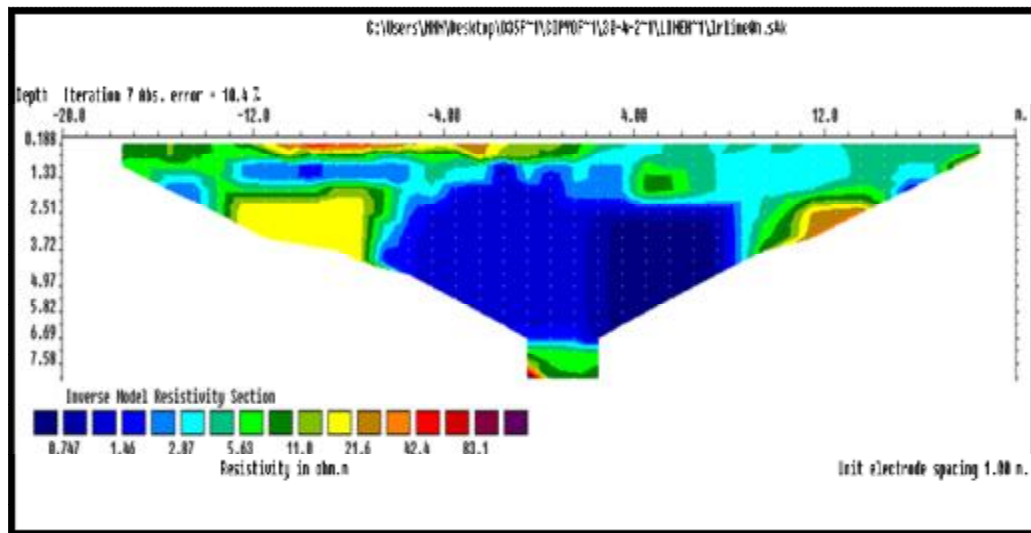
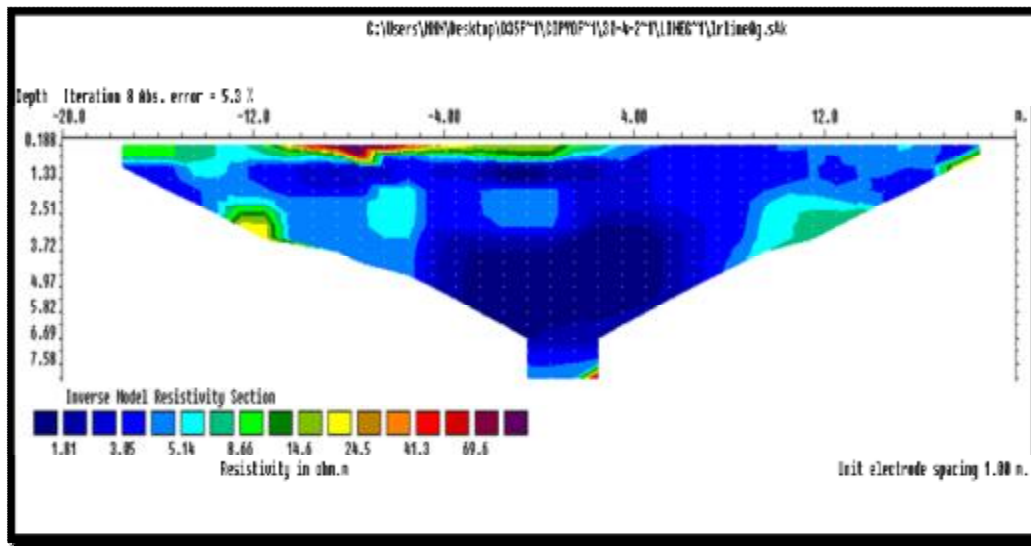


Figure (10) Inverted resistivity section for LINE F.





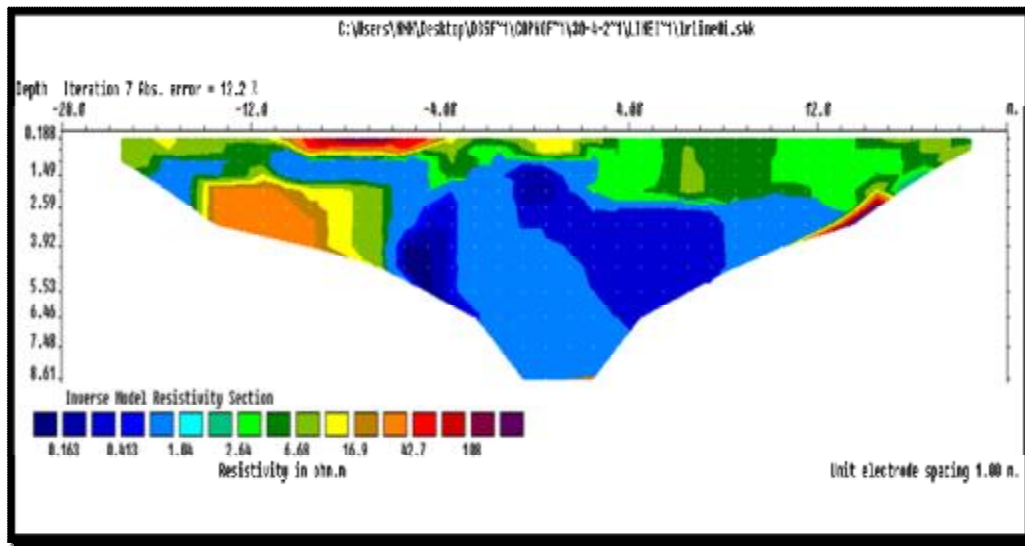


Figure (13) Inverted resistivity section for LINE I.

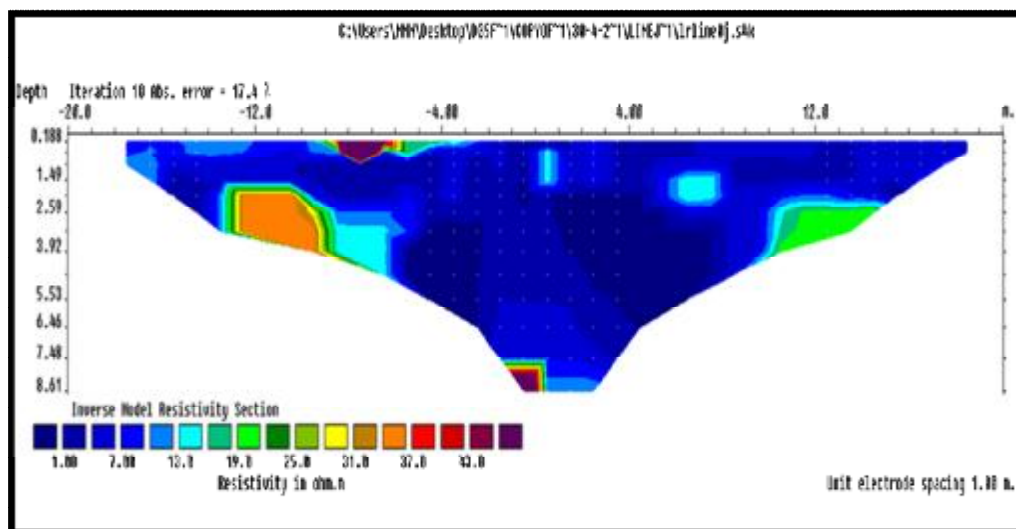


Figure (14) Inverted resistivity section for LINE J.

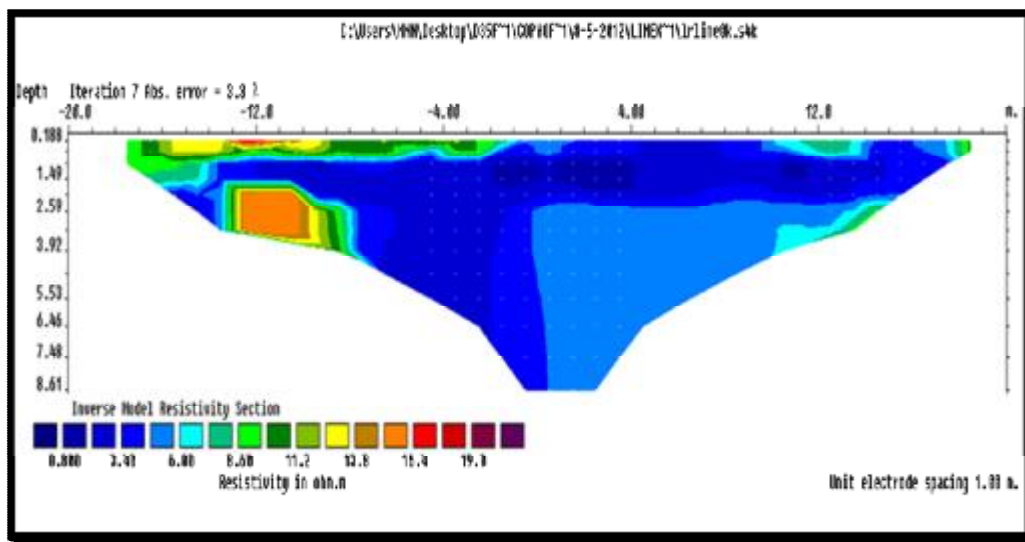


Figure (15) Inverted resistivity section for LINE K.

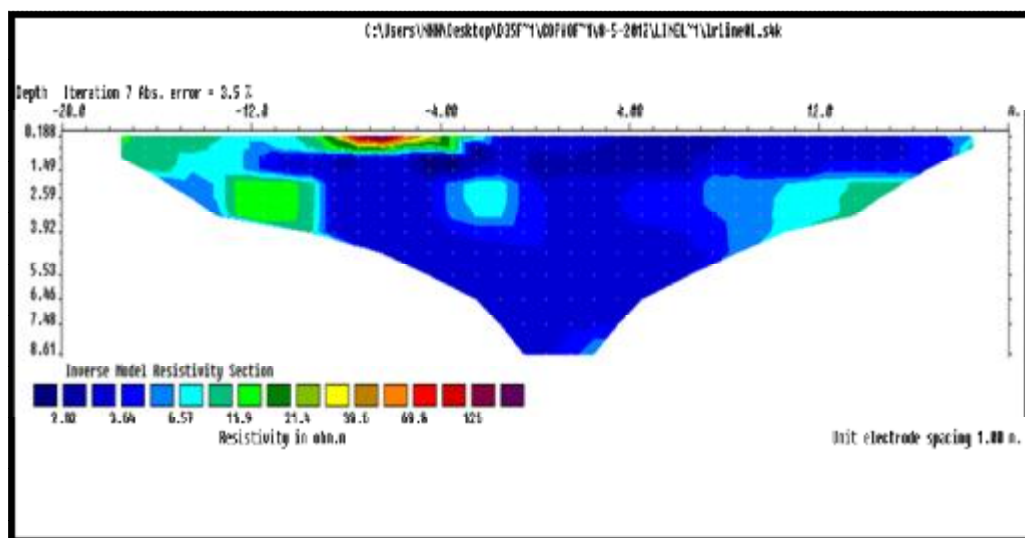


Figure (16) Inverted resistivity section for Line L.

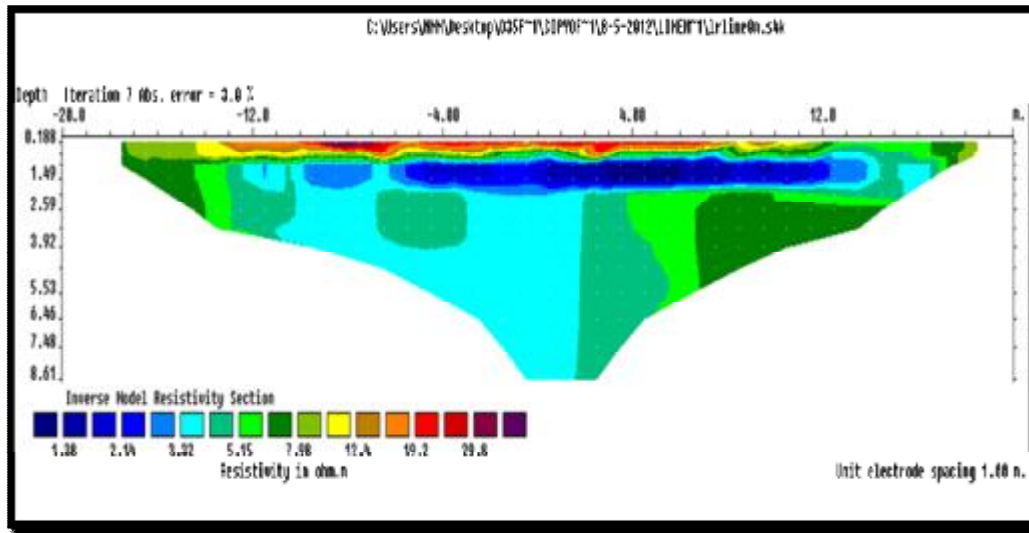


Figure (17) Inverted resistivity section for LINE M.

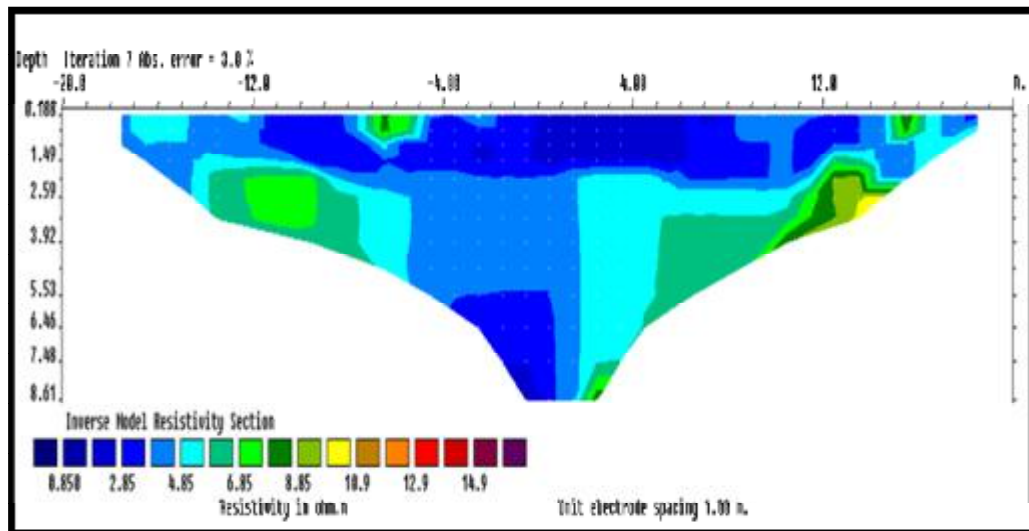
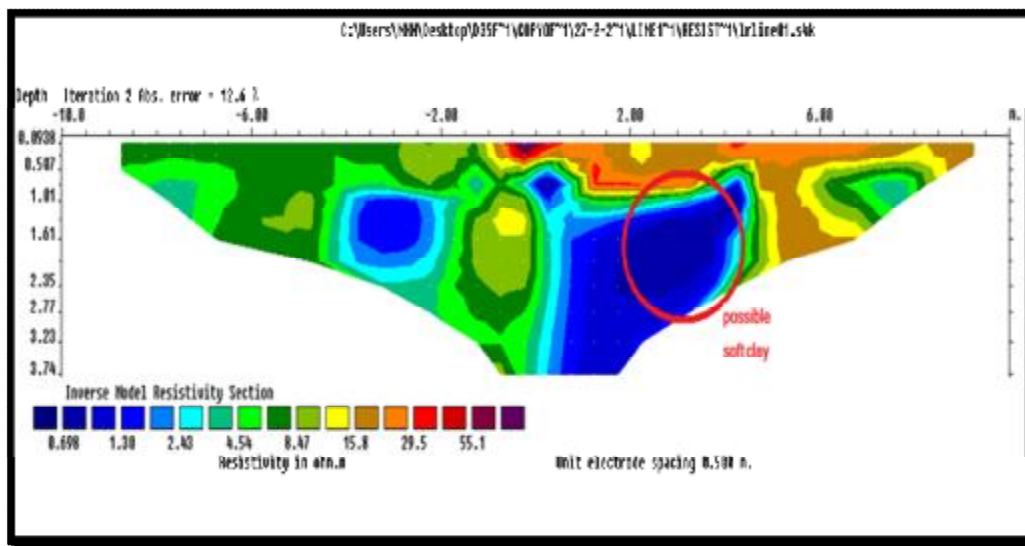
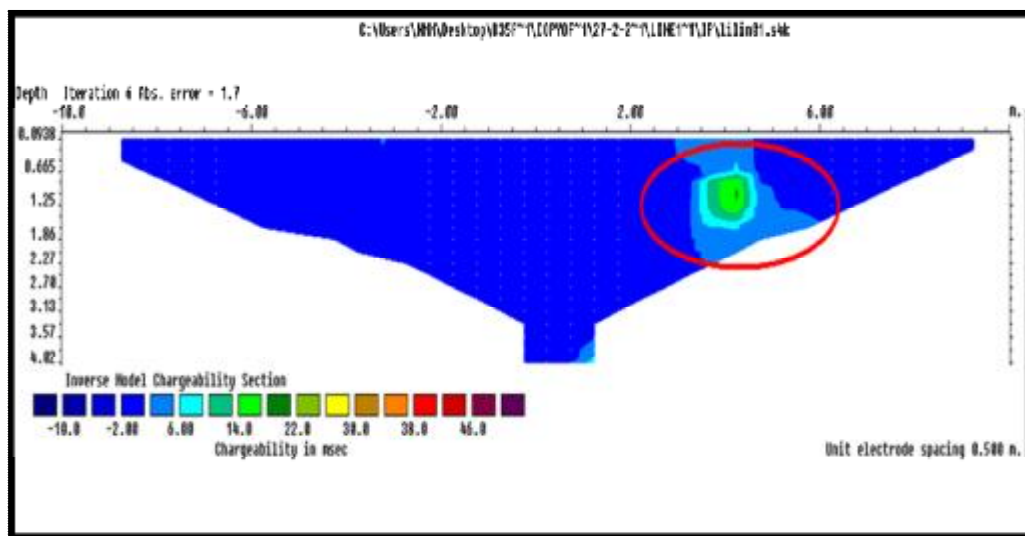


Figure (18) Inverted resistivity section for LINE N.

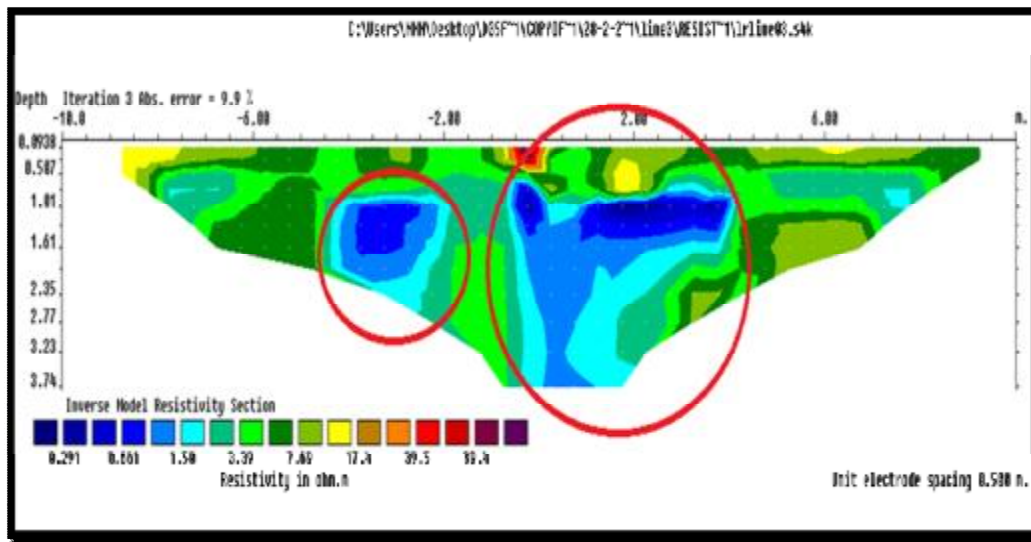


(a)

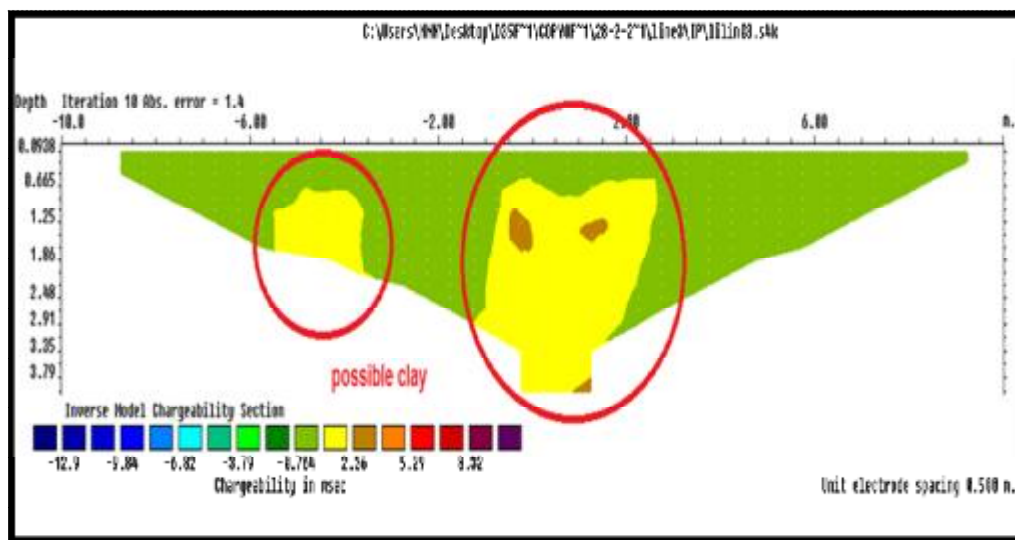


(b)

Figure (19) Inverted sections of LINE 1: (a) resistivity; (b) chargeability.



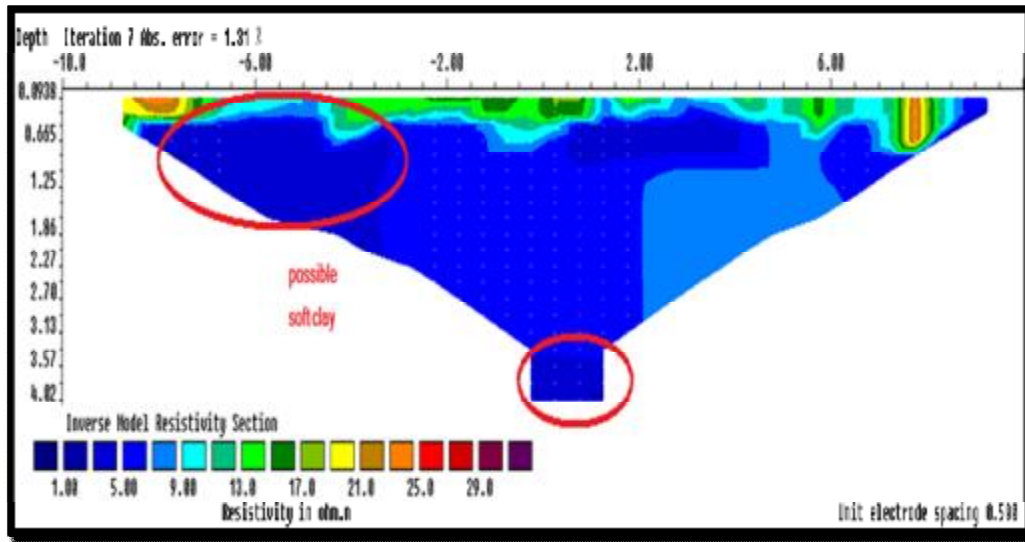
(a)



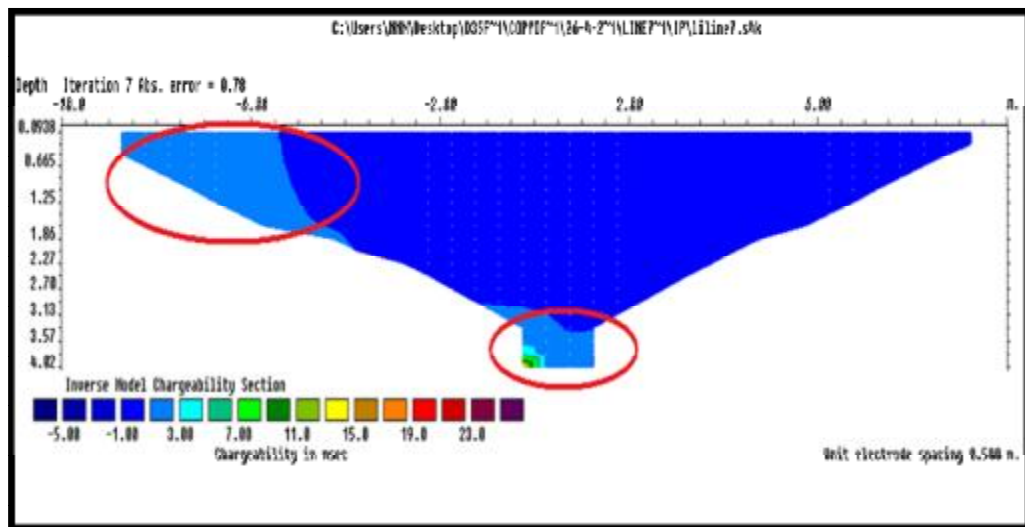
(b)

Figure (20) Inverted sections of LINE 3: (a) resistivity; (b) chargeability.





(a)



(b)

Figure (21) Inverted sections of LINE 7: (a) resistivity; (b) chargeability.

